Proc. of JSCE,
No. 193, September 1971

SNAP-THROUGH BUCKLING OF BLOCKS LAID IN A LINE

*By Masahiro KAWAGUCHI**

I. INTRODUCTION

One of the important problems of concrete pavements is so called blowups. Pavements resist blowups or buckling generally by their bending stiffness and dead load. As the author has previously reported[1], the continuous pavements would scarecely buckle because of their effective stiffness of continuity. Concrete pavements usually needs contraction joints in order to prevent from unfavorable cracks due to shrinkage. It means that the joints separate the pavement in length and reduce the effective bending stiffness. As a result, the pavements with joints may have much greater oppotunity to buckle than continuous pavements. An example of the buckled pavements with joints is shown in Photo1, which was taken by the author on the route No. 8 in Takaoka-city, Toyama Prefecture, August 13, 1970.

In this study the pavements with joints are to be investigated against buckling. Since, practically speaking, the boundary conditions at joints are quite complicated[2], it is necessary to idealize that part in the investigation.

A series of blocks laid in a line was adapted for the studies of the pavements separated by joints. Each block was assumed to have infinitely large stiffness of bending. As for the conditions of connections of each block, the way of rectanguler prism type and that having hinged joints were used. The latter is the simplest statical model of the pavement with joints.

Thus, more informations concerning snap-through phenomena of the pavement with joints, for instance, the upper buckling load was obtained for the first time in the field of this subject.

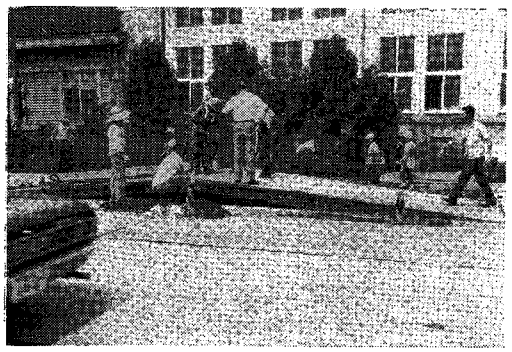

Photo 1 A buckling of pavement with joints took place on the route No. 8 in Takaoka-city, Toyama Prefecture, in the afternoon of August 12,1970.

* Dr. Eng., Assistant Professor, Dept. of Transportation and Traffic Eng., Nihon Univ., Funabashi-shi.

II. SNAP-THROUGH BUCKLING OF BLOCKS LINKED BY HINGED JOINTS

Some theoretical analyses of the buckling of the link have been reported in the previous papers[2),3)]. For simplicity only symmetrical links were treated there. In this report a general type of link is analysed.

(1) Fundamental equations

Let us consider the state of link as shown in Fig. 2.1. It is here assumed that the link has initial imperfection and is affected by elasticity of appara-

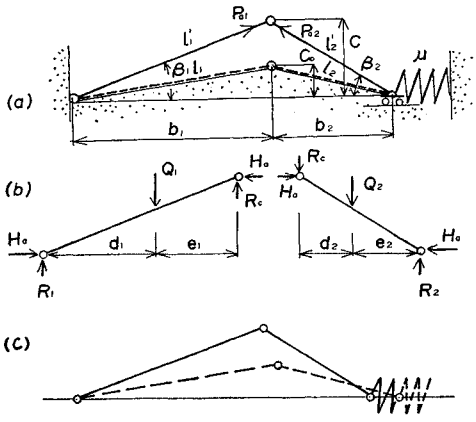

Fig. 2.1 Geometrical characteristics and forces of the link.

tus which is represented by the spring μ in Fig. 2.1. The bending stiffness of the link is also assumed infinitive. The link is restricted to one degree of freedom.

From the equilibrium of the link, the compressive stress resultants of the buckled link are determined as follows : (Notations are listed in Appendix)

$$\left.\begin{aligned} R_1&=\frac{e_1+b_2}{b_1+b_2}Q_1+\frac{e_2}{b_1+b_2}Q_2\\ R_2&=\frac{d_1}{b_1+b_2}Q_1+\frac{b_1+d_2}{b_1+b_2}Q_2\\ H_a&=\frac{b_1}{c}R_1-\frac{e_1}{c}Q_1 \end{aligned}\right\} \cdots\cdots\cdots\cdots (2\text{-}1)$$

$$\left.\begin{aligned} P_{a1}&=H_a\cos\beta_1+R_1\sin\beta_1\\ P_{a2}&=H_a\cos\beta_2+R_2\sin\beta_2 \end{aligned}\right\} \cdots\cdots\cdots\cdots (2\text{-}2)$$

The relation between the axial forces and the horizontal reaction is obtained as follows :

$$H=P_1\frac{l_1}{b_1}=P_2\frac{l_2}{b_2}$$

At the moment of buckling, the variation of axial lengths of the struts may be observed, of which the amount is

$$\begin{aligned}&(l_1'-l_1)+(l_2'-l_2)\\ &=l_1(P_1-P_{a1})/EA+l_2(P_2-P_{a2})/EA \cdots\cdots (2\text{-}3)\end{aligned}$$

where l_1' and l_2' satisfy the following geometrical relation, namely

$$l_1'+l_2'=\sqrt{b_1^2+c^2}+\sqrt{b_2^2+c^2}+(H-H_a)/\mu$$

From these considerations, the equation of unknown displacement c is obtained;

$$\gamma\{(c/b_1)^2-(c_0/b_1)^2\}+(Q_1/EA)(b_1/c)\lambda=P_1/EA \cdots\cdots\cdots\cdots (2\text{-}4)$$

in which c_0 is the initial displacement of the hinge.

To simplify the above equation, following nondimensional terms are introduced; namely,

$$\left.\begin{aligned} &v=c/b_1,\ v_0=c_0/b_1,\ q=Q_1/EA,\ p=P_1/EA,\\ &\gamma=0.5(b_1/l_1)(1+b_1/b_2)\{1+b_2/b_1+EA/\mu\, l_1\cdot l_1/b_1\},\\ &\lambda=b_2/b_1\cdot(d_1/b_1+e_2/b_2\cdot Q_2/Q_1)(b_1/l_1)/(1+b_2/b_1) \end{aligned}\right\} \cdots\cdots\cdots\cdots (2\text{-}5)$$

Consequently, the eq. (2-4) is simplified as

$$\gamma(v^2-v_0^2)+\lambda q/v=p \cdots\cdots\cdots\cdots (2\text{-}6)$$

The axial force after buckling in eq. (2-2) is also expressed as

$$p_a=P_{a1}/EA=\lambda q/v \cdots\cdots\cdots\cdots (2\text{-}7)$$

The total potential energies before and after buckling consist of the strain energies of struts and spring and the potential energy of dead weight; thus

$$\left.\begin{aligned} U&=\frac{P_1^2l_1}{2EA}+\frac{P_2^2l_2}{2EA}+\frac{H^2}{2\mu}+\frac{c_0d_1}{b_1}Q_1+\frac{c_0e_2}{b_2}Q_2\\ U_a&=\frac{P_{a1}^2l_1'}{2EA}+\frac{P_{a2}^2l_2'}{2EA}+\frac{H_a^2}{2\mu}+\frac{cd_1}{b_1}Q_1+\frac{ce_2}{b_2}Q_2 \end{aligned}\right\} \cdots\cdots\cdots\cdots (2\text{-}8)$$

where U and U_a denote the potential energy before and after buckling respectively. The potential energy of the dead weight is zero at the level of $c_0=0$. Nondimensional equations of those energies are as follows :

$$\left.\begin{aligned} u&=U/EAl_1=a_1p^2+a_2qv_0,\\ u_a&=U_a/EAl_1=a_1p_a^2+a_2qv \end{aligned}\right\} \cdots\cdots\cdots\cdots (2\text{-}9)$$

in which

$$a_1=0.5\{1+(b_2/b_1)^2\cdot l_1/l_2+(l_1/b_1)^2\cdot EA/\mu\, l_1\},$$
$$a_2=d_1/l_1+b_1/l_1\cdot e_2/b_2\cdot Q_2/Q_1$$

Initial displacement v_0 acts as initial imperfection at buckling[2].

(2) Calculation of the buckling load

The lower limit of the buckling load p_{cr} and the lower buckling load p_l have been obtained as the critical loads of the link[2),3)]. The lower limit of the buckling load is determined by the condition that the fundamental equation (2-6) has a solution or not (of Fig. 2.2).

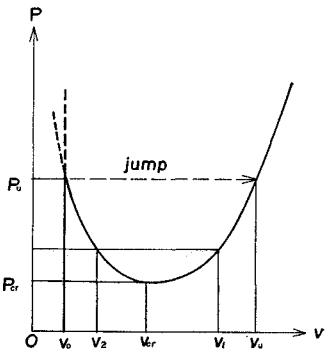

Fig. 2.2 Equilibrium equation of link. $\gamma(v^2-v_0^2)+\lambda q/v=P$

At the extreme point of $v-p$ curve, v is equal to $(\lambda q/2\gamma)^{1/3}$, which is called v_{cr}. Substituting v_{cr} into eq. (2-6), p_{cr} is obtained :

$$p_{cr}=1.89(\gamma\lambda^2q^2)^{1/3}-\gamma v_0^2 \cdots\cdots\cdots\cdots (2\text{-}10)$$

When the initial displacement v_0 is greater than $\sqrt{3}v_{cr}$, p_{cr} is negative, that is, this critical load loses a significance.

In order to determine the lower buckling load p_l, the potential energy is to be considered. When v_0 is smaller than v_{cr}, the relations between p_{cr}, p_l and the upper buckling load p_u can be recognized as shown in Fig. 2.3. Although p_{cr} and p_l have been defined previously by the author, p_u is introduced for the first time in this subject.

The energy difference between u and u_a is calculated to determine p_l,

$$\Delta=a_1(p^2-p_a^2)+a_2q(v_0-v) \cdots\cdots\cdots\cdots (2\text{-}11)$$

Substituting eq. (2-6) and (2-7) into the above p and p_a, the necessary condition for v_l is derived from the criterion of equal energy ($\Delta=0$). As the initial imperfection v_0 is small, the characteristic parameters of the system have the following relation from eq. (2-5) and (2-9) :

$$a_1 r\lambda = a_2/4 \quad \cdots\cdots (2\text{-}18)$$

The energy difference is then derived :

$$\Delta = (v-v_0)^2\{a_1 r^2 v(v+v_0)^2 - 0.5\, a_2 q\}/v \quad \cdots\cdots (2\text{-}13)$$

In order to obtain $v_l (>v_0)$ from $\Delta=0$, the following relation must be satisfied :

$$a_1 r^2 v_0 (v_0+v_0)^2 - 0.5\, a_2 q < 0$$

then,

$$v_0 < (\lambda q/2r)^{1/3} = v_{cr}$$

Substituting the solution v_l into eq. (2-6), the lower buckling load p_l is obtained. The mechanical system can buckle if it is supplied with energy gap r' in Fig. 2.3. This critical load has been used in designing shell structure.

The upper buckling load is derived :

$$p_u = \lambda q/v_0 \quad \cdots\cdots (2\text{-}14)$$

The displacement of upper buckling v_u is calculated by eq. (2-6). Only the upper buckling load is to be called, in a strict sense, the critical load, because the system jumps at p_u without any supply of energy as shown in Fig. 2.3.

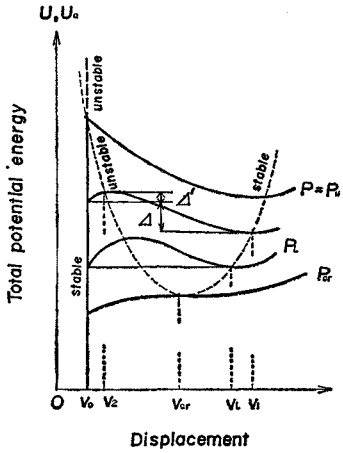

Fig. 2.3 Total potential energy of the link for given compressive force.

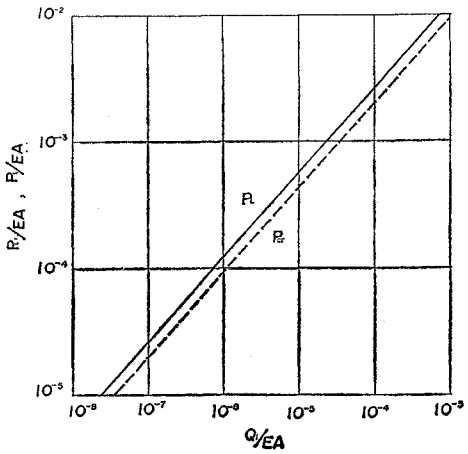

Fig. 2.4 Critical loads versus dead load ($EA/\mu l_1=0.0$, $b_2/b_1=1.0$ $C_0/b_1=0.0$).

When v_0 is equal to v_{cr}, the three critical loads p_{cr}, p_l and p_u are all equal. If v_0 is over v_{cr}, p_l can not be obtained.

The results of the above calculations are shown in Figs. 2.4···, 2.9. From those results the follow-

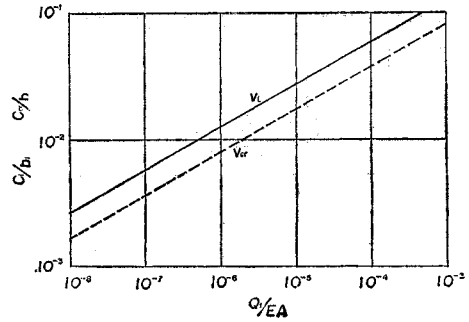

Fig. 2.5 Buckling displacements versus dead load ($EA/\mu l_1=0.0$, $b_2/b_1=1.0$, $C_0/b_1=0.0$).

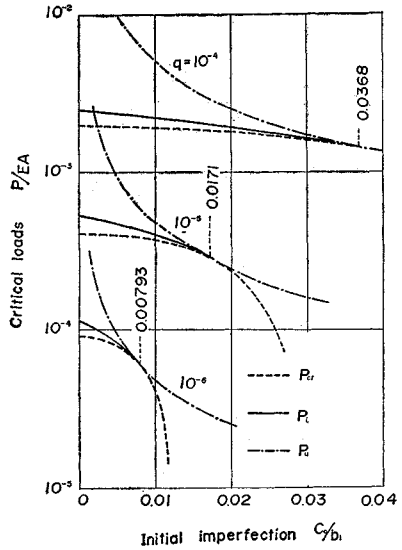

Fig. 2.6 Effect of initial imperfection on critical loads ($EA/\mu l_1=0.0$, $b_2/b_1=1.0$).

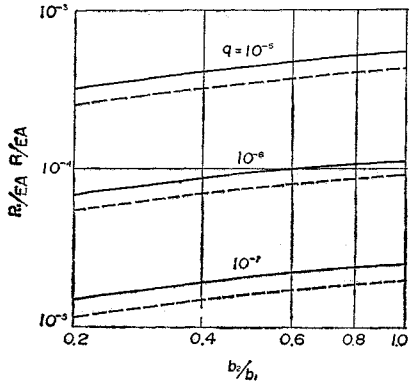

Fig. 2.7 Mode of link—Critical loads (solid line=p_l, dotted line=p_{cr}). ($EA/\mu l_1=0.0$, $C_0/b_1=0.0$)

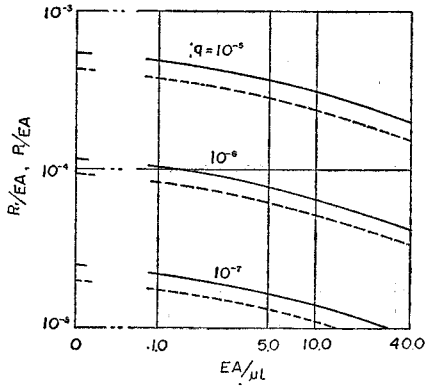

Fig. 2.8 Effect of stiffness of apparatus on critical loads (solid line=p_l, dotted line=P_{cr}). $b_2/b_1=1.0$, $C_0/b_1=0.0$.

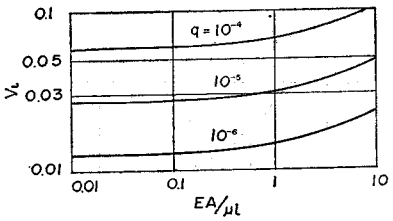

Fig. 2.9 Effect of stiffness of apparatus on displacement of lower buckling.

ing considerations follow :

1) p_{cr} and p_l are in proportion to q^x, where x is near to 2/3 for $b_2/b_1=1.0$;

2) v_{cr} and v_l are in proportion to q^y, where y is near to 1/3 for $b_2/b_1=1.0$;

3) Though the initial imperfection has little effect on p_l if it is less than a certain value, it diminishes p_u very much;

4) The unsymmetrical buckling mode is more likely to occur than symmetrical one;

5) p_{cr} and p_l decrease and v_l increases with decreasing stiffness of apparatus.

III. SNAP-THROUGH BUCKLING OF BLOCKS OF RECTANGULAR PRISM

The system of blocks of rectangular prisms is an idealized model of the pavement with joints. The actual boundary conditions are supposed to have intermediate characteristics between this system and the pin jointed link which was treated in chapter II.

(1) Fundamental equations

The system of the blocks is composed of two blocks of different lengths and a spring as shown in Fig. 3.1. Each block has infinite bending stiffness and the buckled blocks have such geometrical characteristics as shown in Fig. 3.1.

The compressive stress resultants of the buckled

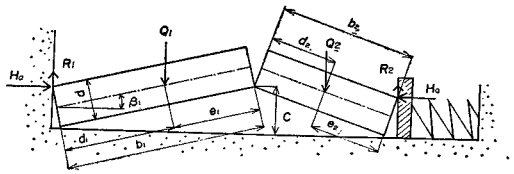

Fig. 3.1 System of blocks of rectangular prisms of which bending stiffness is infinitive. b_1, b_2, d_1, d_2, e_1 and e_2 are lengths before buckling.

blocks are determined from the equilibrium as in II. The horizontal reaction after buckling denoted by H_a is derived from momentum equilibrium of the left block :

$$H_a=\frac{\lambda Q_1}{c/b_1-d/b_1} \quad \cdots\cdots(3\text{-}1)$$

The compressive stress resultants after buckling are obtained by neglecting the components of R_1 and R_2.

$$P_{a1}=H_a\cos\beta_1,\quad P_{a2}=H_a\cos\beta_2 \quad \cdots\cdots(3\text{-}2)$$

The compatibility equation is derived as follows:

$$\begin{aligned} b_1+b_2-(P-H_a)/\mu=d(\sin\beta_1+\sin\beta_2)\\ +b_1\{1+(P-P_{a1})/EA\}\cos\beta_1\\ +b_2\{1+(P-P_{a2})/EA\}\cos\beta_2 \end{aligned} \quad \cdots\cdots(3\text{-}3)$$

From the above equations, the fundamental equation is obtained in the nondimensional form :

$$\left.\begin{aligned} &\gamma v(v-2d)+\lambda q/(v-d)=p\\ &p_a=\lambda q/(v-d)\\ &d=d/b_1 \end{aligned}\right\} \quad \cdots\cdots(3\text{-}4)$$

If d is equal to zero, eq. (3-4) is equal to eq. (2-6), which is concerned with the link without initial imperfection.

As a next step, the total potential energies before and after buckling are to be derived. They consist of the strain energies of the blocks and the spring of apparatus and the potential energy of the dead weight.

$$\left.\begin{aligned} &u=a_1p^2\\ &u_a=a_1p_a^2+a_2qv \end{aligned}\right\} \quad \cdots\cdots(3\text{-}5)$$

(2) Energy consideration

As in case of the link, it is necessary to consider the energy change of buckling blocks. From those considerations the buckling criterion may be derived.

The following data are used for numerical calculations :

$$a_1=0.5(1+b_2/b_1)=a_2$$

This means that there is no spring effect of apparatus, both of blocks have the same density and the centers of gravity are at the center of each block.

For q-value, 10^{-7}, 10^{-5}, 10^{-3} are used. The value for concrete pavements is between 10^{-6} and 10^{-5}.

When q is small or d is large, $p-v$ curve may sink below v-axis as shown in Fig. 3.2(b). In this

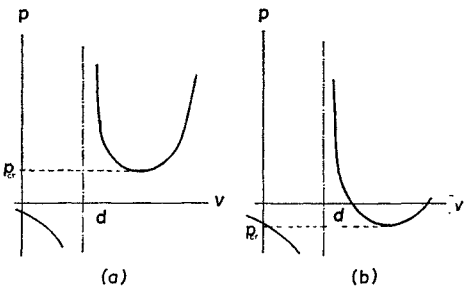

Fig. 3.2 Equilibrium equation of buckled system of blocks; $\gamma' v(v-2d)+\lambda' q/(v-d)=p$

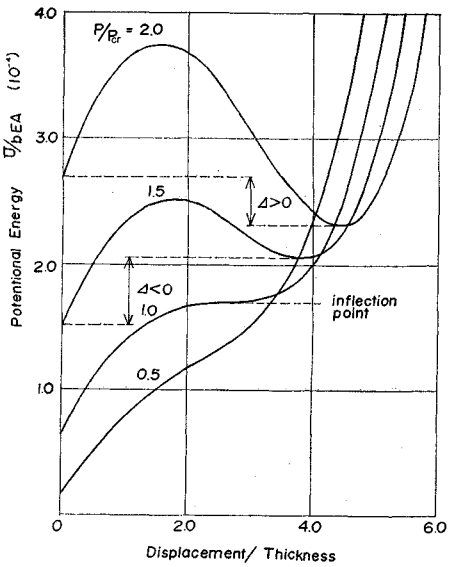

Fig. 3.3 Potential energy of the system of blocks versus displacement.

case the extreme $p(=p_{cr})$ is negative. The potential energy reaches an inflection point at this p_{cr}. Then if p_{cr} is negative, the energy curve has not any inflection point, because the compressive force must be positive.

The case of positive p_{cr} is shown in Fig. 3.3. It is observed that this potential curve of buckling blocks has essentially the same characteristics as one of the buckling link (Fig. 2.3). When p is smaller than p_{cr}, the curve has not any extreme value. If p is equal to p_{cr}, it has an inflection point The curve may not have two extreme points till p increases over p_{cr}. The curve has stable equilibrium state at the extreme point of larger displacement, but the energy of the system without displacement $(v=v_0)$ is less than the one of this equilibrium states, if p is not enough large. This is shown in Fig. 3.3 for $p=1.5\,p_{cr}$. Then the blocks do not buckle for $1.5\,p_{cr}$. For larger compressive force, for example $2.0\,p_{cr}$, u increases above u_a and the system may buckle, if it can go over the energy peak with a kind of excitation. This is the equal energy criteria of snap-through buckling. It is important that the energy is also minimum at $v=0$ and the state of no displacement is stable. The upper limit or the true critical load can not be obtained.

The energy curves for negative p_{cr} change more steeply than the curves for positive p_{cr}. The energy curves for unsymmetrical blocks are steeper than those for symmetrical blocks. And they change in high-pitch according to increasing relative thickness of blocks.

(3) Calculation of the critical loads

From the above considerations the critical loads are obtained by the same methods used in II. The lower limit of the buckling load is calculated from the condition that eq. (3-4) has any non-trivial solution. As shown in Fig. 3.2, v must be greater than d. The extreme point is calculated:

$$\frac{dp}{dv}=\gamma(2v-2d)-\lambda q/(v-d)^2=0$$

The critical displacement v_{cr} is obtained;

$$v_{cr}=d+(\lambda q/2\gamma)^{1/3} \quad \cdots\cdots (3\text{-}6)$$

By introducing v_{cr} into (3-4), the lower limit of the buckling load p_{cr} is derived;

$$p_{cr}=\gamma v_{cr}(v_{cr}-2d)+\lambda q/(v_{cr}-d) \quad \cdots\cdots (3\text{-}7)$$

The difference of the potential energy before and after buckling is denoted by Δ.

$$\Delta=a_1(p^2-p_a{}^2)-a_2qv \quad \cdots\cdots (3\text{-}8)$$

The lower buckling displacement v_l is obtained from the equal energy criterion:

$$\Delta(v_l)=0 \quad \cdots\cdots (3\text{-}9)$$

This algebraic equation is to be solved numerically. Then the lower buckling load is

$$p_l=\gamma v_l(v_l-2d)+\lambda q/(v_l-d) \quad \cdots\cdots (3\text{-}10)$$

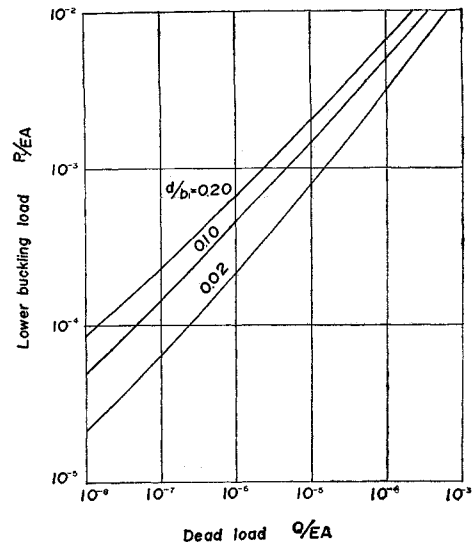

Fig. 3.4 Lower buckling load $(EA/\mu l_1=0,\ b_2/b_1=1.0)$.

The upper limit p_u can not be obtain without initial imperfection.

The results of calculations are shown in Fig. 3.4, ···, 3.7. From those figures following considerations follow :

1) The lower buckling load of the block system is rather larger than one of the link system. p_l is almost in proportion to q^n, where n is about 0.5.

2) The buckling displacement is very large comparing with one of the linked blocks.

3) The symmetrical system and the unsymmetrical have nearly equal lower buckling load.

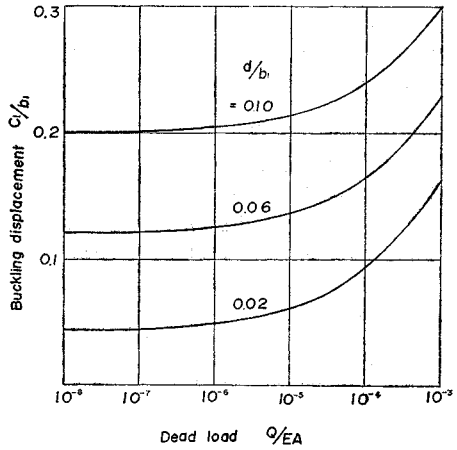

Fig. 3.5 Buckling displacement versus dead load ($EA/\mu l_1=0$, $b_2/b_1=1.0$).

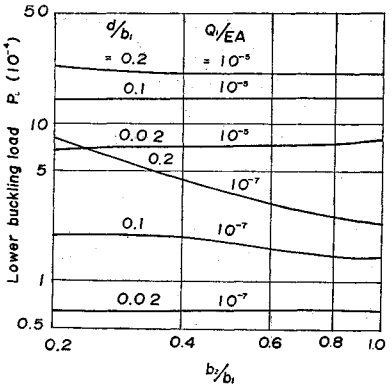

Fig. 3.6 Effect of unsymmetricity on buckling loads.

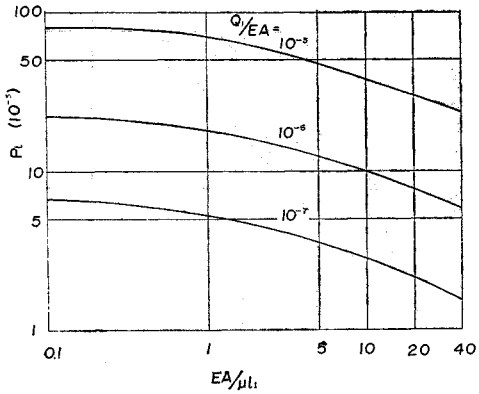

Fig. 3.7 Effect of stiffness of apparatus on buckling load ($b_2/b_1=1.0$, $d/b_1=0.02$).

IV. EXPERIMENTS

Experiments were carried out in order to verify the numerical calculations. In the experiments wood blocks and steel edges were used. As shown in Fig. 4.1, each rectangular prism of wood had a knife edge or a flat edge. A knife edge of a block and a flat edge of the next block constructed a hinged joint. Two flat edges contacting each other were assembled into the blocks mentioned in Ⅲ.

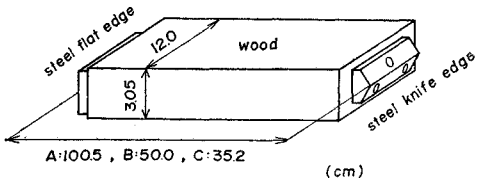

Fig. 4.1 Experimented wood block.

Blocks were 3.05 cm thick and 12.0 cm wide. The lengths of the blocks of wood part were 98.0 cm, 48.0 cm and 33.0 cm and they were called A-type, B-type and C-type in the order of length. Young's modulus of elasticity of wood was measured 1.2×10^5kg/cm^2 by bending test. The wood was sufficiently elastic. Weights of specimens were 1 716 g for A_1, 1 943 g for A_2, 1 114 g for B_1 and B_2, 860 g for C_1, C_2 and C_3. The center of gravity of each block was nearly at the center of each block.

The experimental apparatus was the same one used before[1]. The compressive force was applied with an oil jack and the force was measured with a ring dynamometer. The experiments were conducted for many cases : various combinations of A, B and C-blocks, different orders of those blocks and some cases with turned over blocks.

Photos 2, 3, 4, 5 and 6 show the experimented

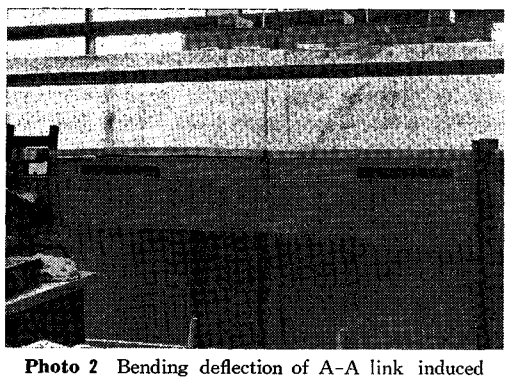

Photo 2 Bending deflection of A-A link induced by eccentric compression.

specimens. Photo 2 shows a bending blocks of linked A–A system, which was compressed at 1 820 kg and could no longer be stressed on the threat of bending buckling. In this case so called Euler buckling load of strut of the block with hinged boundary condition was about 3 250 kg. Then the bending deflection was considered to be induced by eccentric compression.

Photo 3 shows a buckling hinged C–C system of blocks. This picture was taken with a stroboscope. A contact switch and wire can be seen at the left of the photo.

Photo 4 shows one of the buckling C–B systems. The blowup occurred at compressive force of 256 kg. The stroboscope flashed a little bit after buckling, then the two blocks had been already apart at the top of peak. Photo 5 is the other case of a buckled C–B system which blowed up violently at 2 000 kg. When the system resisted large compressive force, the buckling occurred violently and the relatively light wood blocks fled off. On the other hand the system rised quietly for small buckling load.

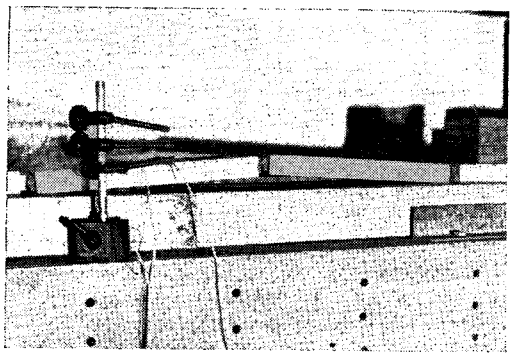

Photo 3 Buckling hinged C–C system of blocks.

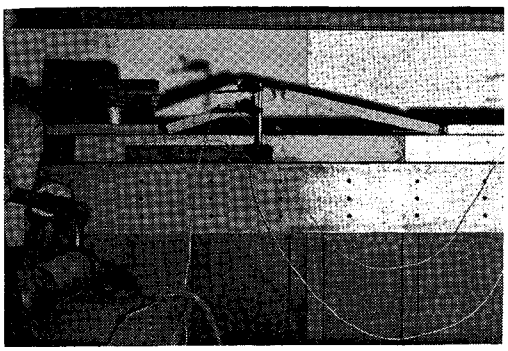

Photo 4 Buckling C–B system at compressive force of 256 kg.

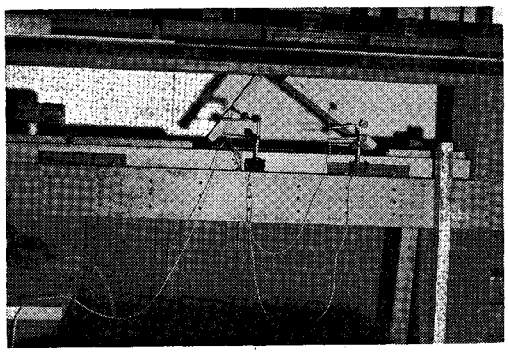

Photo 5 C–B system which blowupped violently at 2 000 kg.

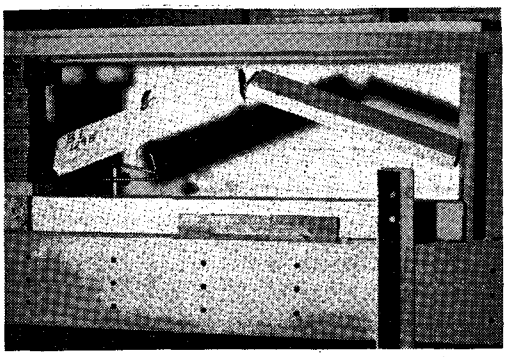

Photo 6 Extremely violent buckling of C–C type with only flat edges.

The above mentioned experiments were carried out for hinged blocks. The block systems with only flat edges treated in Ⅲ were too strong to buckle experimentally. Photo 6 shows such extremely violent buckling of C–C type. Wood screws, which set the edges to wood blocks, were subjected to tensile forces and then became loose at buckling. Consequently accurate experimental results could not be obtained. Therefore in this chapter only hinged blocks were treated

The knife edges were not attached ideally at the centers of the sections of blocks, but they were shifted up or down vertically or they were attached inclined. The eccentricities of knife edges were measured 0.5 mm at maximum. And the relative eccentricity[3] between one joint and the other could be supposed to consist of each imperfection of edges and apparatus. Maximum relative imperfections were supposed 0.64 mm for A–A type, 0.31 mm for B–B, 0.78 mm for A–B, 0.78 mm for A–C, 0.64 mm for B–C, 0.47 mm for C–C, and 0.50 mm for apparatus respectively.

The spring of the apparatus consisted of the wood blocks which remained level without buckling, and the ring dynamometer which had spring constant of 1.37×10^{4}kg/cm.

The theoretical values of p_l and p_u, which were calculated in consideration of the above imperfections and the spring constant, are shown in Fig. 4. 2 in comparison with the experimental results. The experimental results scattered very remarkablly. It was considered that the initial imperfections affected the buckling load very much. Although all of

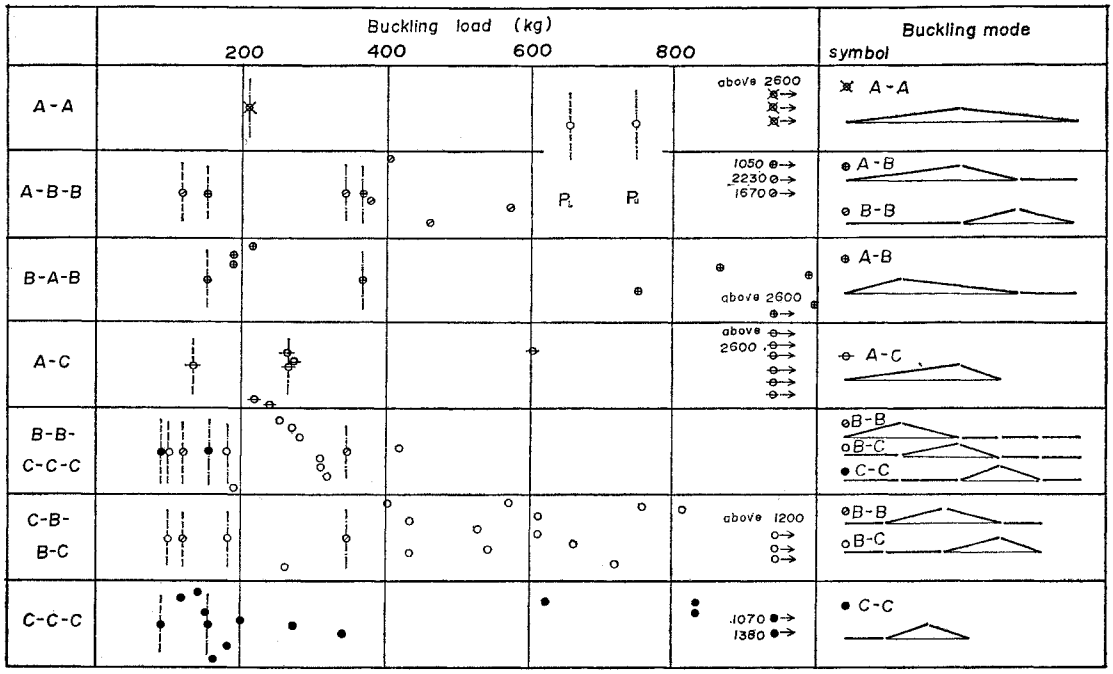

Fig. 4.2 Experimental buckling loads put down in order of experiments. P_u were calculated in consideration of initial imperfection; 1.14 mm for A-A and B-C, 0.81 mm for B-B, 1.28 mm for A-B and A-C, 0.97 mm for C-C. There were some experimental results below the calculated P_u for B-A-B, A-C and C-C-C, however all of them were above P_l.

the results were above the calculated p_l, there were some which were below the calculated upper buckling load.

In order to observe effectiveness of the initial imperfection, the link of B-B type was tested for given imperfection. Those imperfections were introduced by wedges of known thicknesses which were inserted under the link. Those results are shown in Fig. 4.3. It is seen that the upper buckling load p_u is the most valuable in case of imperfections and the lower buckling load is also meaningful for $v_0 \leq v_{cr}$.

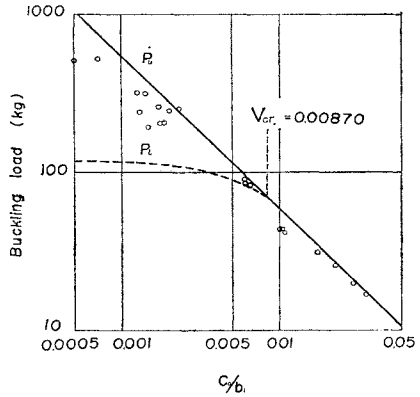

Fig. 4.3 Effect of initial imperfection of buckling load. Theoretical curves ane experimental results.

V. CONCLUSIONS

Statical systems of linked blocks or rectangular prisms, which were assumed idealized models of the pavement with joints, were studied experimentally as well as theoretically.

Buckling phenomena of those compressed systems were snap-through. As for the snap-through buckling of the systems, the following conclusions are derivde :

1) The lower buckling load derived by equal energy criterion is always lower than the experimental buckling load;

2) The upper buckling load is calculated for the linked system with initial imperfection. The system has bifurcation phenomena and jumps at $p=p_u$;

3) The initial imperfections slightly decrease the lower buckling load, but they remarkablly reduce the experimented buckling load and the theoretical upper buckling load p_u. This p_u is meaningful for the system with initial imperfection;

4) Unsymmetrical buckling mode is more likely to occur than symmetrical one;

5) Systems of rectangular prisms are more resistive to buckling than linked blocks.

ACKNOWLEDGMENT

The author would like to thank his colleague Mr.

Y. Miura for his encouragement and advices, Mr. S. Kawano for his contributions to the experiments and Mr. H. Kimura for his kindness in drawing the figures of manuscript.

This work was financially supported by Nihon University.

The numerical works were carried out at the Computer Center of University of Tokyo.

NOTATION

b_1, b_2=horizontal lengths of blocks;
c=distance from level to buckled state;
c_0=initial imperfection of link;
d=depth of blocks or the ratio of d and b_1;
d_1, d_2, e_1, e_2=distances from centers of gravity to ends of blocks (see Fig. 2.1);
l_1, l_2=lengths of bolcks;
p, $p_a=P_1/EA$, P_{a1}/EA;
$q=Q_1/EA$;
p_{cr}, p_l, $p_u=P_{cr}/EA$, P_l/EA, P_u/EA;
u, $u_a=U/EAl_1$, U_a/EAl_1;
v, $v_0=c/b_1$, c_0/b_1;
EA=stiffness of block;
H, H_a=horizontal force before and after buckling respectively;
P_1, P_2, P_{a1}, P_{a2}=compressive stress resultants before and after buckling;
P_{cr}=lower limit of the buckling load;
P_l=lower buckling load;
P_u=upper buckling load;
U, U_a=total potential energy before and after buckling respectively;
$\beta_i=\sin^{-1}c/l_i$;
$\Delta=u-u_a$;
γ, λ=nondimensional characteristic terms of the system (see eq. 2-5); and
μ=spring stiffness of apparatus (kg/cm).

REFERENCES

1) Kawaguchi, M.: Thermal Buckling of Continuous Pavement, Proc. of JSCE, No. 170, Oct., 1969, pp. 37-52 (in Japanese), and Transactions JSCE, Vol. 1, Part 2, 1969, pp. 331-344 (in English).
2) Kawaguchi, M.: Experiments on the Buckling of Blocks Laid in a Line, Proc. of JSCE, No. 180, Aug. 1970, pp. 91-95 (in Japanese).
3) Kawaguchi, M.: Snap-through Buckling of Link Laid on Rigid Floor, Proc. of JSCE, No. 177, May, 1970, pp. 59-62 (in Japanese).

(Received Dec. 14, 1970)

昭和三十七年五月二十八日印刷
昭和四十六年九月十五日発行
昭和四十六年九月二十日発行
（毎月一回二十日発行）
郵便物認可

土木学会論文報告集 第193号

土木計測用 ひずみゲージ式 変換器

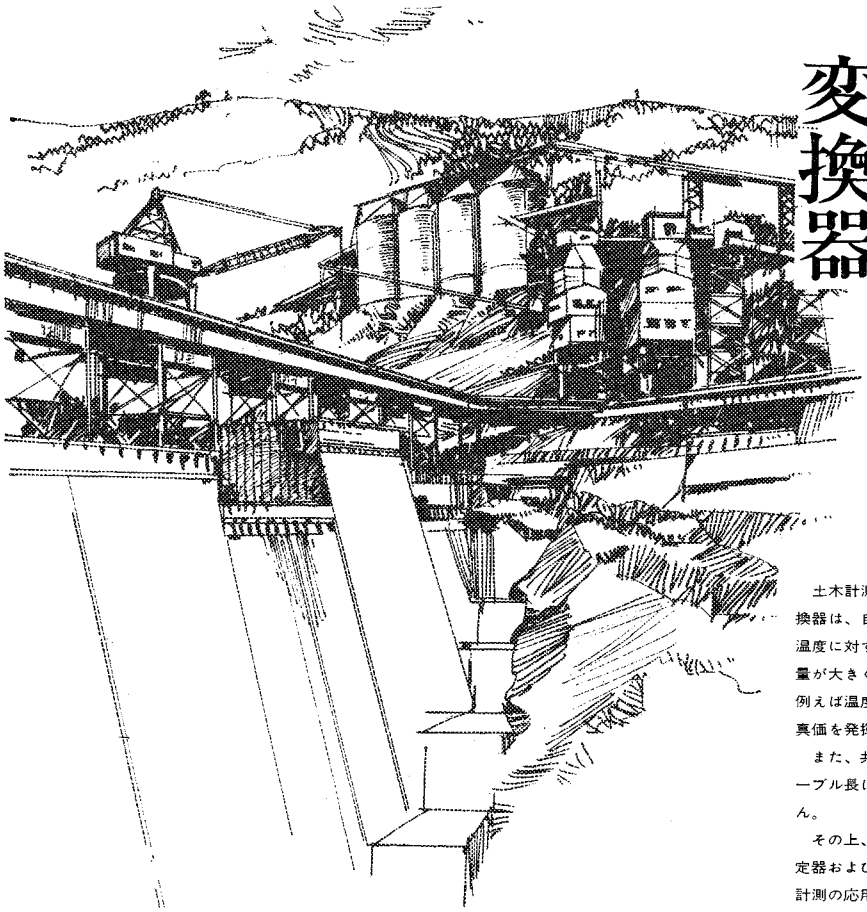

土木計測用に開発されたひずみゲージ式変換器は、自己温度補償の原理を取り入れて、温度に対する補正が不要になりました。補正量が大きく真値のつかみにくい場での計測、例えば温度変化の大きい場などで使用すれば、真価を発揮します。

また、共和独特の指示器の採用により、ケーブル長は5kmまで感度に全く影響ありません。

その上、市販されているすべてのひずみ測定器およびその周辺器が使用できますので、計測の応用範囲が広がり便利になりました。

特長

- ●温度補正はいりません
- ●ケーブル抵抗の補正は5kmまで全く不要
- ●あらゆるひずみ測定器に接続できる
- ●小型の構造物にも使える
- ●耐環境性にすぐれ、信頼性が高い

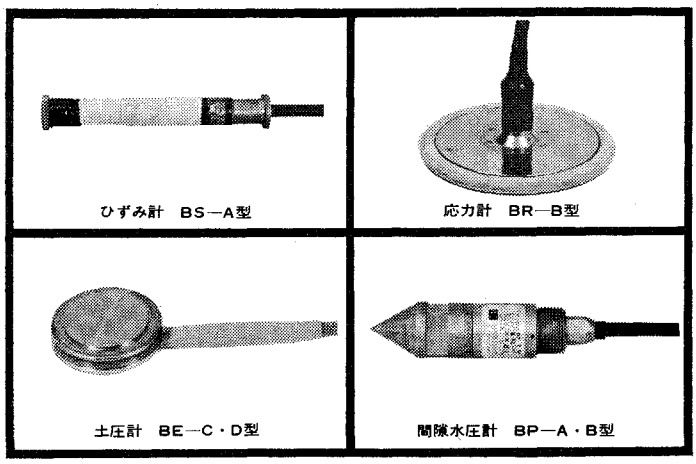

ひずみ計 BS—A型

応力計 BR—B型

土圧計 BE—C・D型

間隙水圧計 BP—A・B型

種類

品名	型式名	容量
ひずみ型	BS－A型	±500×10⁻⁶ひずみ
応力計	BR－B型	20, 50, 100kg/cm²
間隙水圧計	BP－A型	2,5,10,20kg/cm²
	BP－B型	2,5,10,20kg/cm²
土圧計	BE－B型	2,5,10kg/cm²
	BE－C型	2,5,10kg/cm²
	BE－D型	2,5,10kg/cm²
	BE－E型	2,5,10,20kg/cm²
	BE－F型	2,5,10,20kg/cm²
変位変換器	BCD 型	± 5 mm

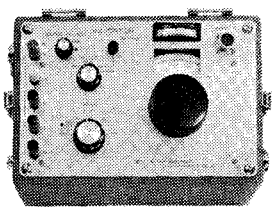

専用指示器 BM—12A

●カタログお送りいたします。
誌名記入のうえ広報係まで

土木計測器の専門メーカー
共和電業
本社・工場 東京都調布市下布田1219
電話 東京調布0424—83—5101
営業所／東京・大阪・名古屋・福岡・広島・札幌 出張所／水戸

定価三五〇円